2015 IEEE International Conference on Robotics and Automation (ICRA)
Washington State Convention Center
Seattle, Washington, May 26-30, 2015

Robust Adaptive Control of Quadrotor Unmanned Aerial Vehicle with Uncertainty

S. Islam, M. Faraz, R. K. Ashour, J. Dias, L. D. Seneviratne

***Abstract*— In this paper, we deal with the stability and tracking control problem of quadrotor unmanned aerial vehicle (UAV) in the presence of the modeling error and disturbance uncertainty. The flight tracking control system combines classical proportional-derivative (PD) like term with robust and adaptive control term. Lyapunov method is used to design and show the asymptotic behavior of the linear and angular states of the vehicle. In contrast with other existing adaptive backstepping design, the proposed design is very simple and easy to implement as it does not require multiple design steps without using augmented signals and known bound of the uncertainty. Various experimental results on quadrotor UAV system are presented to demonstrate the effectiveness of the proposed design for real-time application.**

***Index Terms*— Quadrotor Unmanned Aerial Vehicle; Lyapunov Method; Robust Adaptive Control.**

I. Introduction

Recently, more and more researchers and industrial companies have focused their attention on designing a new type of small scale unmanned aerial vehicles. The interest in such small scale vehicles is growing in military and civilian applications, such as surveillance, inspection, search and rescue missions in dangerous or hostile environment. The design of autonomous flight control system for small scale quadrotor UAV in the presence of uncertainty is very difficult tasks due to its inherent nonlinearity associated with the dynamical model, underactuated property and external disturbances associated with uncertain flying environment. Over the past years, various automatic flight control systems for quadrotor system have been reported in the literature [2-6, 8-20]. Among these designs, PID and LQR type classical control mechanism has been widely used for commercial quadrotor system [4, 5, 8, 10, 11, 19, 23]. These classical algorithms may exhibit poor hovering performance because of the modeling error uncertainty. Backstepping control technique has been proposed to address the problem associated with the modeling error dynamics of the vehicle in [12, 15, 16, 17, 18]. Later, in [13], author included integral action with the backstepping technique in order to minimize the steady state tracking error. Most quadrotor unmanned flying robots are usually very small and lightweight, making the system sensitive to the variation in payload and uncertainty. This means that additional payload mass, moment of inertia, aerodynamic and gyroscopic force may change vehicles dynamic, affecting the stability and tracking performance significantly. Furthermore, unpredictable changes in flying environment may increase the modeling error and uncertainty, making the flight control system design even more complicated. As a result, available classical flight control system may not be able to deal with the change in flight dynamics for different flight missions. Therefore, the problem associated with uncertainty remains a challenging task demanding advanced autonomous flight control design for quadrotor UAV system. To deal with above mentioned problem, nonlinear control technique has been employed for UAV system in [2, 3, 6, 9, 20]. In [2], authors have proposed so called dynamic inversion mechanism for hovering flight control system design by using well-known feedback linearization technique. H_∞ control technique combined with backstepping control mechanism in [6]. Nonlinear adaptive control algorithms using the backstepping technique proposed in [9]. Most recently, adaptive backsteeping control algorithm technique used to design nonlinear control for quadrotor UAV systems [3, 21]. However, the design and implementation mechanism of existing nonlinear control algorithms are very complicated as they usually associated with augmented auxiliary signals requiring multiple design and computation steps.

In this paper, we propose nonlinear robust control for stability and tracking control of quadrotor UAV system in the presence of uncertainty. Our aim in this work is to develop very simple flight control strategy which can cope with modeling error and disturbance uncertainty. Virtual position control algorithm combines gravity compensation with the desired linear acceleration and PD like error term. Attitude controller comprises PD like error term with the desired angular acceleration term. Adaptation laws are used in both position and attitude dynamics to learn and compensate uncertainty associated with the variation of the payload mass, inertia, aerodynamic and gyroscopic force, external disturbance and unpredictable change in outdoor flying environment. Lyapunov method is employed to design control algorithm and to analyze the convergence property of the linear and angular state dynamics. Unlike existing methods, the design does not use augmented signals and multiple design steps which makes the design very simple and easy to implement for practical applications. Moreover, the design does not require *a priori* known bound of the uncertainty. Finally, various experimental results on actual quadrotor UAV system are presented to demonstrate the effectiveness of the proposed method for practical applications. This paper

S. Islam is with University of Ottawa, Canada, Carleton University, Canada, and KUSTAR, Abu Dhabi, 1027788 UAE.
M. Faraz is with KUSTAR, Abu Dhabi, 1027788 UAE.
R. K. Ashour is with KUSTAR, Abu Dhabi, 1027788 UAE.
J. Dias is with University of Coimbra, Portugal and KUSTAR, Abu Dhabi, 1027788 UAE.
L. D. Seneviratne is with Kings College London, UK, and KUSTAR, Abu Dhabi, 1027788 UAE.

is organized as follows. We begin the paper by introducing kinematic and dynamic model of the system in section II. In section II, we also introduce robust control strategy. A detail stability analysis is given in section II. Experimental results are presented in section III. Finally, conclusion is given in section IV.

II. Model Dynamics, Algorithm Design and Stability Analysis

We first derive mathematical model of the quadrotor UAV system [12, 13]. The position of the vehicle is defined by $P(t) = [x(t)\ y(t)\ z(t)]^T$ and its attitude represented by three Euler angles as $\Theta(t) = [\phi(t)\ \theta(t)\ \varphi(t)]^T$. The three translational and rotational velocities are defined as $V(t) = [V_1(t)\ V_2(t)\ V_3(t)]^T$ and $\Omega(t) = [\Omega_1(t)\ \Omega_2(t)\ \Omega_3(t)]^T$, respectively. Then, the relationship between velocities $(\dot{P}, \dot{\Theta}(t))$ and (V, Ω) can be written for earth fixed inertial reference frame and body fixed frame attached to the vehicle as follows

$$\dot{P} = \mathcal{R}_t(\Theta)V, \Omega = \mathcal{B}(\Theta)\dot{\Theta} \tag{1}$$

where $\mathcal{R}_t \in \Re^{3\times3}$ and $\mathcal{B} \in \Re^{3\times3}$ are the transformation velocity matrix and the rotation velocity matrix between fixed inertial frame and body fixed frame as given as follows

$$\mathcal{R}_t = \begin{bmatrix} C_\phi C_\varphi & S_\phi S_\theta C_\varphi - C_\phi S_\varphi & C_\phi S_\theta C_\varphi + S_\phi S_\varphi \\ C_\theta S_\varphi & S_\phi S_\theta S_\varphi + C_\phi C_\varphi & C_\phi S_\theta C_\varphi - S_\phi S_\varphi \\ -S_\phi & S_\phi C_\theta & C_\phi C_\theta \end{bmatrix} \tag{2}$$

$$\mathcal{B} = \begin{bmatrix} 1 & 0 & -S_\theta \\ 0 & C_\phi & C_\theta S_\phi \\ 0 & -S_\phi & C_\phi C_\theta \end{bmatrix} \tag{3}$$

where $S_{(.)}$ and $C_{(.)}$ denote $\sin(.)$ and $\cos(.)$, respectively. We now take the derivative equation (1) to constitute the kinematic equations for the quadrotor vehicle

$$\ddot{P} = \mathcal{R}_t\dot{V} + \dot{\mathcal{R}}_t V \tag{4}$$

$$\dot{\Omega} = \mathcal{B}\ddot{\Theta} + \left(\frac{\partial \mathcal{B}}{\partial \phi}\dot{\phi} + \frac{\partial \mathcal{B}}{\partial \theta}\dot{\theta}\right)\dot{\Theta} \tag{5}$$

Using $\dot{\mathcal{R}}_t = \mathcal{R}_t S(\Omega)$ with the skew-symmetric matrix $S(\Omega)$

$$S(\Omega) = \begin{bmatrix} 0 & -\Omega_3 & \Omega_2 \\ \Omega_3 & 0 & -\Omega_1 \\ -\Omega_2 & \Omega_1 & 0 \end{bmatrix} \tag{6}$$

we can write equation (4) and (5) in the following form

$$\ddot{P} = \mathcal{R}_t\left(\dot{V} + \Omega \times V\right) \tag{7}$$

$$\dot{\Omega} = \mathcal{B}\ddot{\Theta} + \mathcal{D}(\Theta, \dot{\Theta}) \tag{8}$$

with

$$\mathcal{D}(\Theta, \dot{\Theta}) = \begin{bmatrix} -C_\theta\dot{\theta}\dot{\varphi} \\ -S_\phi\dot{\phi}\dot{\theta} + C_\phi C_\theta\dot{\phi}\dot{\varphi} - S_\phi S_\theta\dot{\theta}\dot{\varphi} \\ -C_\phi\dot{\phi}\dot{\theta} - S_\phi C_\theta\dot{\phi}\dot{\varphi} - C_\phi S_\theta\dot{\theta}\dot{\varphi} \end{bmatrix} \tag{9}$$

The dynamic equation of motion for the vehicle subjected to forces U_f and moments U applied to the center of the mass can be derived as

$$\ddot{P} = \beta U_f - \mathcal{C}\dot{P} - \gamma \tag{10}$$

$$\ddot{\Theta} = \mathcal{M}U - \eta\mathcal{D}(\Theta, \dot{\Theta}) - \xi\dot{\Theta} - \mathcal{B}\dot{\Theta} \times \mathcal{B}I\dot{\Theta} - \mathcal{B}\dot{\Theta} \times \Sigma_{i=1}^{4} I_r\omega_i \tag{11}$$

where U_f is the force generated by the propellers, U is the total moments developed by the propellers, $\mathcal{M} = (I\mathcal{B})^{-1}$, $\eta = \mathcal{B}^{-1}$, $\beta = \left(m\mathcal{R}_t^T\right)^{-1}$ with constant payload mass m, $\mathcal{C} = m^{-1}L$ with aerodynamic drag coefficients $L = diag\,[L_{d1},\ L_{d2},\ L_{d3}]$ with $L_{d1} > 0$, $L_{d2} > 0$ and $L_{d3} > 0$, $\gamma = TH$ with $T = [0, 0, 1]^T$, $H = [0\ 0\ g\ ]^T$ and $g = 9.81\frac{m}{s^2}$, I_r is the inertia of the rotor blade, ω_i are the angular velocities of the rotors and $\xi = I^{-1}M$ with symmetric positive definite constant inertia matrix $I = diag[I_x, I_y, I_z]$ and aerodynamic coefficients $M = diag\,[M_1,\ M_2,\ M_3]$ $M_1 > 0$, $M_2 > 0$ and $M_3 > 0$. Let us now introduce robust flight control strategy for the quadrotor UAV system given by equation (10) and (11). It is assumed that the translational and rotational dynamics are affected by external disturbance uncertainties as defined as $F_a(t) = [F_x(t), F_y(t), F_z(t)]^T$ and $F_b(t) = [F_\phi(t), F_\theta(t), F_\psi(t)]^T$. We also assume that the desired task x_{1d}, x_{3d} and their first and second derivatives are bounded and belongs to a known compact set. Throughout our stability analysis, the position, orientation and their first derivatives are assumed to be available for measurement. Since $-\frac{\pi}{2} < \phi < \frac{\pi}{2}$, $-\frac{\pi}{2} < \theta < \frac{\pi}{2}$ and $-\pi < \psi < \pi$, the matrices $\mathcal{R}_t$ and $\mathcal{B}$ are bounded as $\|\mathcal{R}_t\| \leq k_r$ with $k_r > 0$ and $\|\mathcal{B}\| \leq k_t$ with $k_t > 0$. Then, we develop robust flight control algorithm for the attitude, altitude and virtual position dynamics such that (ϕ, θ, ψ) and (x, y, z) converges to the desired $(\phi_d, \theta_d, \psi_d)$ and (x_d, y_d, z_d). To do that, lets define the following state variables for the position and attitude dynamics as $x_1 = P$ and $x_3 = \Theta$. Then, the error model can be presented by the following state space equation

$$\dot{e}_1 = e_2, \dot{e}_2 = -\beta U_f + \gamma + \mathcal{C}x_2 - F_a + \ddot{x}_{1d}$$

$$\dot{e}_3 = e_4, \dot{e}_4 = -\mathcal{M}U - \zeta + \ddot{x}_{2d} \tag{12}$$

where $U_f = \mathcal{U}_t$, $\zeta = f(x_3, x_4) + F_b$, $f(x_3, x_4) = -\eta\mathcal{D}(x_3, x_4) - \xi x_4 - \mathcal{B}x_4 \times \mathcal{B}Ix_4 - \mathcal{B}x_4\Sigma_{i=1}^{4} I_r\omega_i$, $e_1 = (x_{1d} - x_1)$, $e_2 = (\dot{x}_{1d} - \dot{x}_1)$, $e_3 = (x_{2d} - x_3)$ and $e_4 = (\dot{x}_{2d} - \dot{x}_3)$. Then, robust control algorithm for $\mathcal{U}_t$ is designed as follows

$$\mathcal{U}_t = \beta^{-1}(\ddot{x}_{1d} + \mathcal{Y} - \hat{\theta}_L sign^T(S_L))$$

$$\dot{\hat{\theta}}_L = \Gamma_1 sign(S_L)S_L^T \tag{13}$$

where $S_L = e_a^T P_L B_1$ with positive definite matrix P_L to be determined later, $\mathcal{Y} = (k_1x_2 + S_1 + \gamma)$, $S_1 = (k_{p1}e_1 + k_{d1}e_2)$, $\hat{\theta}_L$ is the estimate of the bound of the signals F_a, $k_1 = diag[k_{11}, k_{12}, k_{13}]$, $k_{p1} = diag[k_{p11}, k_{p2}, k_{p3}]$, $k_{d1} = diag[k_{d1}, k_{d2}, k_{d3}]$, $\Gamma_1 > 0$, $B_1 = [0; I]$, $e_a =$

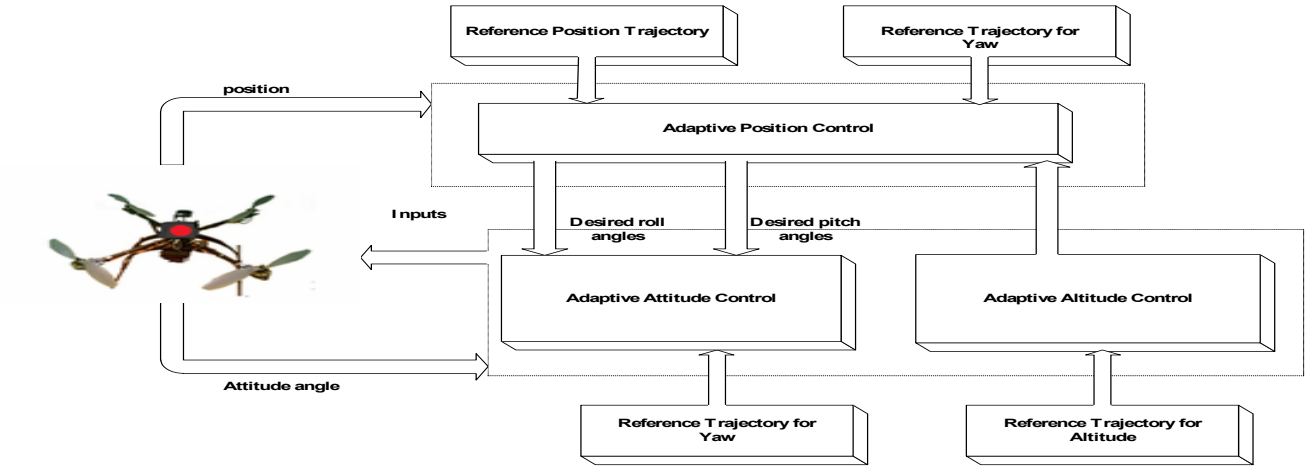

Fig. 1. Experimental setupb of the proposed design.

$[e_1^T,\ e_2^T]^T$ and $\mathcal{U}_t = [\mathcal{U}_{t1}, \mathcal{U}_{t2}, \mathcal{U}_1]^T$. Robust control algorithm for $\mathcal{U}$ can be designed as follows

$$\begin{aligned} \mathcal{U} &= \mathcal{M}^{-1}\left(\ddot{x}_{2d} + S_2 - \hat{\theta}_A sign^T(S_A)\right) \\ \dot{\hat{\theta}}_A &= \Gamma_2 sign(S_A) S_A^T \end{aligned} \tag{14}$$

where $S_A = e_b^T P_A B_2$ with positive definite matrix P_A to be determined later, $S_2 = (k_{d2}e_4 + k_{p2}e_3)$, $\hat{\theta}_A$ is the estimate of the bound γ_d, $k_{p2} = diag[k_{p21}, k_{p22}, k_{p23}]$, $k_{d2} = [k_{d21}, k_{d22}, k_{d23}]$, $\Gamma_2 > 0$, $B_2 = [0;\ I]$, $e_b = [e_3^T,\ e_4^T]^T$ and $\mathcal{U} = [\mathcal{U}_2, \mathcal{U}_3, \mathcal{U}_4]^T$. It is well-known that the learning estimate used in (13) and (14) may exhibit discontinuity [1, 7] demanding projection based mechanism as [14] $\dot{\hat{\theta}}_L = Proj\left(\theta_L, \Gamma_1 sign(S_L) S_L^T\right)$ and $\dot{\hat{\theta}}_A = Proj\left(\theta_A, \Gamma_2 sign(S_A) S_A^T\right)$. For algorithm design, stability and tracking convergence analysis, we consider the composite Lyapunov function as defined as $V = \frac{1}{2}e_a^T P_L e_a + \frac{1}{2}\tilde{\theta}_L^T \Gamma_1^{-1} \tilde{\theta}_L^T + \frac{1}{2}e_b^T P_A e_b + \frac{1}{2}\tilde{\theta}_A^T \Gamma_2^{-1} \tilde{\theta}_A^T$ with $\tilde{\theta}_L = (\theta_L - \hat{\theta}_L)$, $\tilde{\theta}_A = (\theta_A - \hat{\theta}_A)$, $A_a^T P_L + P_L A_a = -L_1$ and $A_b^T P_A + P_A A_b = -L_2$ with $A_a = [0\ I; -k_{p1} - k_{d1}]$, $A_b = [0\ I; -k_{p2} - k_{d2}]$. By differentiating V with respect to time along with the tracking trajectory of the closed loop systems derived by equation (12), (13) and (14) with projection mechanism, $\dot{V}$ can be written as $\dot{V} \leq -\frac{1}{2}{N_M}^T L N_M$ with $N_M = [e_a^T, e_b^T]^T$ and $L = [L_1\ 0; 0\ L_2]$. Then, in view of Lyapunov theory together with Barbalat's Lemma [22] and projection mechanism [14], we can conclude that the linear and angular states in the closed loop system are bounded and asymptotically stable as the time goes to infinity.

III. Design Synthesis and Experimental Results

In section, we experimentally tested the proposed design on an actual quadrotor UAV system which has a height of 8cm, wingspan of 55cm and a weight of 500 grams including battery. The payload of the system is 200 gram and can fly about 20 minute. Like other existing method, it is essential in our implementation to decompose robust control design into two loops as inner and outer loop. The attitude dynamics runs on-board microprocessor at about 1 KHz. The angular velocity of the vehicle is measured by on-board gyros. The on-board accelerometer and gyros data is processed at about 300 Hz. The communication between ground and on-board computer is done by Zigbee. To measure altitude of the vehicle, we use on-board barometric pressure sensor. The position of the vehicle in outdoor flying environment is measured by GPS. We use visual tracker provided by Phonenix Technologies Inc. to measure the position of the vehicle in indoor environment. Let us first conduct simulation studies on the given quadrotor UAV system. Our aim in simulation

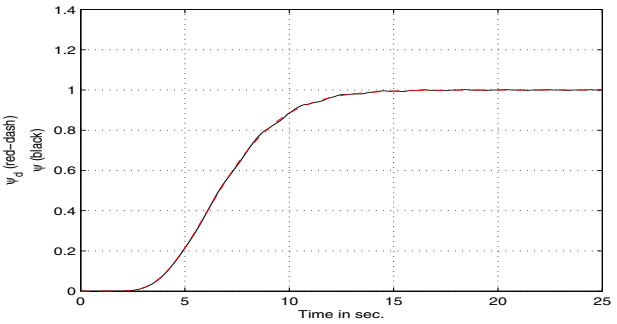

Fig. 2. Desired yaw angle task ψ_d (red-solid line) and actual output ψ (black-dash line) in radians.

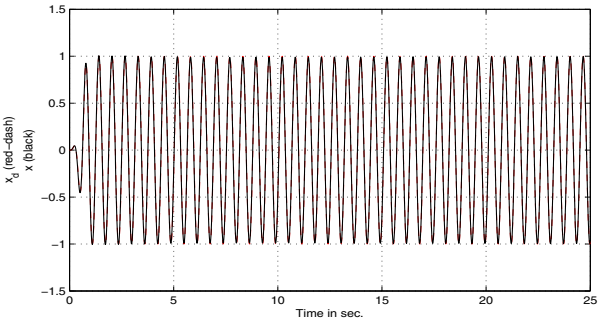

Fig. 3. Desired position tracking x_d (red-solid line) and actual output x (black-dash line) in meters.

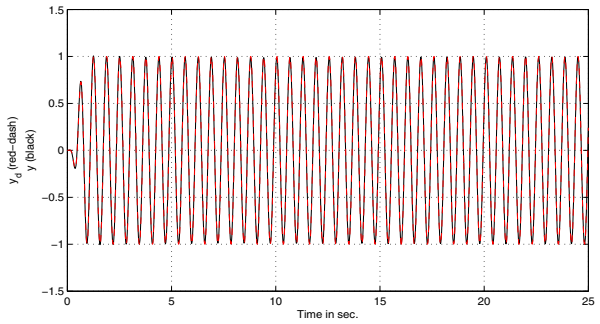

Fig. 4. Desired position tracking y_d (red-solid line) and actual output y (black-dash line) in meters.

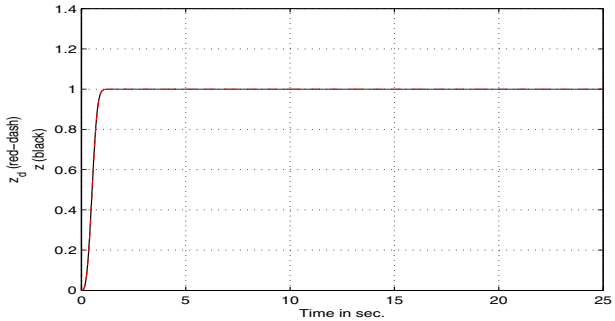

Fig. 5. Desired altitude tracking z_d (red-solid line) and actual output z (black-dash line) in meters.

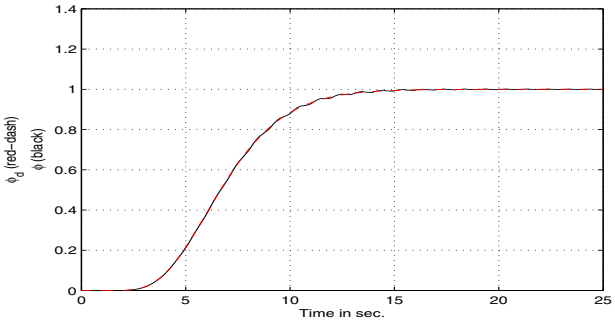

Fig. 6. Desired rolling angle ϕ_d (red-solid line) and actual output ϕ (black-dash line) in radians.

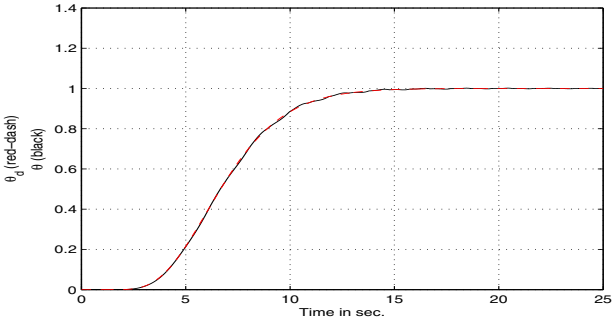

Fig. 7. Desired pitch angle θ_d (red-solid line) and actual output θ (black-dash line) in radians.

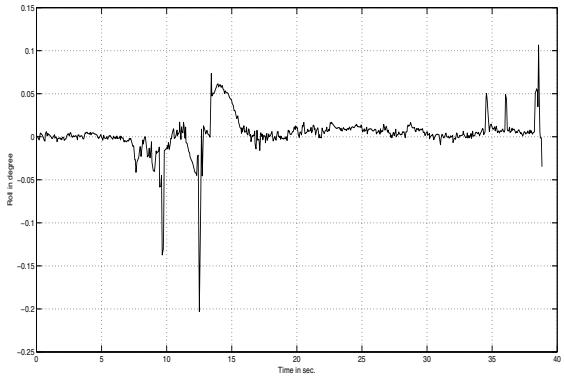

Fig. 8. Figure shows roll angle ϕ in indoor flying environment.

study is to determine the design parameters for experimental evaluation. These evaluation results are based on the dynamic model represented by equation (10) and (11). The parameters of the systems are selected as payload mass $m = 5\ kg$, distance from the center of the mass to the rotor axes $d = 0.2\ m$, lift constant $\alpha = 3.5 \times 10^{-5}\ N.\frac{s^2}{rad^2}$, $g = 9.81\ m.s^{-2}$, the drag factor $\alpha_d = .0032\ Nm.\frac{s^2}{rad^2}$, $I_x = 2\ Nm.\frac{s^2}{rad}$, $I_y = 3\ Nm.\frac{s^2}{rad}$, $I_z = 5\ Nm.\frac{s^2}{rad}$, $L_{d1} = 2\ N.\frac{s}{m}$, $L_{d2} = 5\ N.\frac{s}{m}$, $L_{d3} = 6\ N.\frac{s}{m}$, $M_1 = 3\ Nm.\frac{s}{rad}$, $M_2 = 5\ Nm.\frac{s}{rad}$ and $M_3 = 3\ Nm.\frac{s}{rad}$. Note that we choose the mass and inertial parameters four times larger than the actual values of the parameter of the vehicle making large modeling error uncertainty to ensure that the selected design parameters can deal with large modeling error uncertainty. The translational and rotational air velocities are chosen as $[2, 2, 2]^T$ m/s and $[2, 2, 2]^T$ rad/s. The inertia parameters are fluctuated from 2 to 3, 3 to 4 and 3 to 4 in gm^2, respectively. The values of θ_L and θ_A are varied between -3 Newton to 4 Newton and -3 Newton-meter to 4 Newton-meters. With these design parameters, we first evaluate linear PD like control terms in (13) and (14). Then, we integrate adaptive term with the linear PD like control term. The experimental block diagram representation of the proposed design is shown in Fig. 1. Based on our several simulation studies, we obtain the design parameters as $k_{p1} = diag[25\ 25\ 25]$, $k_{d1} = diag[25\ 25\ 25]$, $k_1 = diag[25\ 25\ 25]$, $k_{p2} = diag[50\ 50\ 50]$, $k_{d2} = diag[50\ 50\ 50]$, $L_1 = L_2 = I$ and $\Gamma_1 = \Gamma_b = 1$. Using with these parameter setup, we apply the proposed design to track the desired trajectories for x_d, y_d and z_d as $x_d(t) = \left(1 - e^{-5t^3}\right) sin(10t)m$, $y_d(t) = \left(1 - e^{-5t^3}\right) cos(10t)m$, $z_d(t) = \left(1 - e^{-5t^3}\right) m$ and $\psi_d = \frac{1}{(s+1)^6}$. The desired roll, ϕ_d, and pitch angle, θ_d, is generated from the relationship $\phi_d = arcsin\left(\mathcal{U}_{t1}\sin(\psi_d) - \mathcal{U}_{t2}\cos(\psi_d)\right)$ and $\theta_d = arcsin\left(\frac{\mathcal{U}_{t1}\cos(\psi_d) + \mathcal{U}_{t2}\sin(\psi_d)}{\cos(\psi_d)}\right)$. The evaluation results are depicted in Figs. 2 to 7. In view of these results, we can see that the linear and angular position of the flying vehicle converges to the reference linear and angular position even in the presence of large modeling error and disturbance uncertainty. Let us now experimentally test attitude control performance

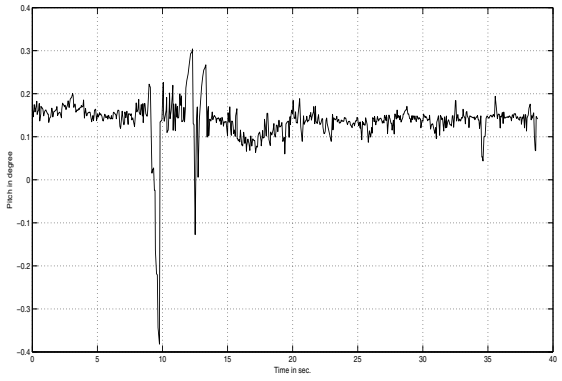

Fig. 9. Figure shows pitch angle θ in indoor flying environment.

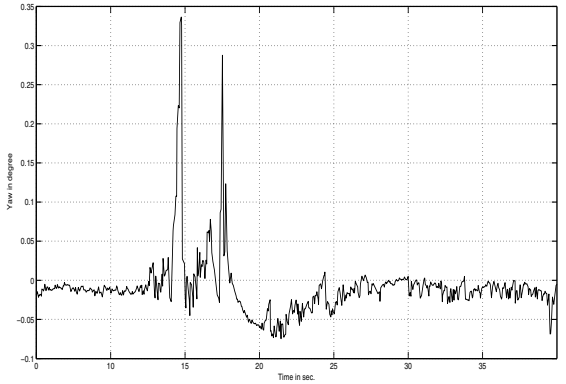

Fig. 10. Figure shows yaw angle ψ in indoor flying environment.

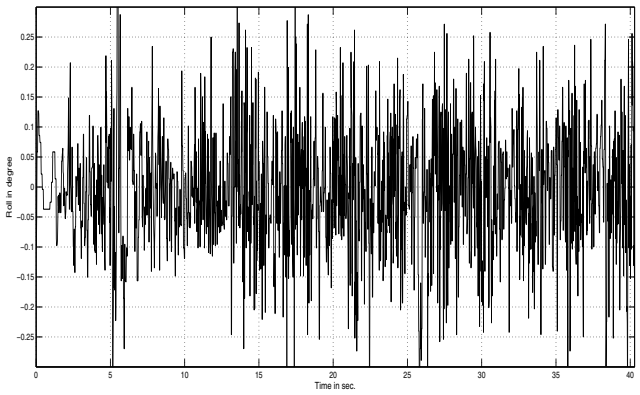

Fig. 11. Figure shows roll angle ϕ in outdoor flying environment.

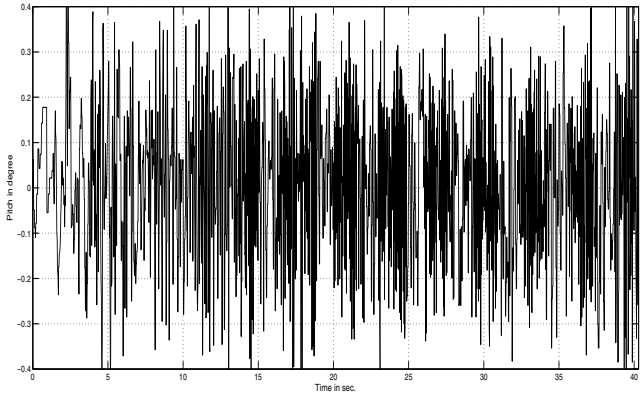

Fig. 12. Figure shows pitch angle output θ in outdoor flying environment.

for quadrotor stability. This is very important because attitude control performance directly related to the performance of the actuators as, in practice, the motor may suffer from bandwidth saturation and slow dynamics under uncertainty as opposed to the assumption of fast dynamics of the actuator. So, our aim is to stabilize the attitude dynamics of the quadrotor in both indoor and outdoor flying environment under free flight mission. The experimental results in indoor flying environment are shown in Figs. 8 to 10. During this experiment, we perturbed the system by injecting external disturbance along ϕ, θ and ψ direction approximately at 9 sec. and 13 sec., 9 sec. and 13 sec. and 13 sec. and 17 sec. respectively. In view of these results, we can notice that roll, pitch and yaw angles are returned almost closed to zero after short transient period. We now test attitude control in outdoor flying environment in the presence of strong wind disturbance uncertainty. The experimental results are shown in Figs. 11 to 13. From these results, we can see that the roll, pitch and yaw angles are stabilized closed to zero under strong external wind disturbance uncertainty. We now experimentally test the proposed design to track a desired position trajectory in indoor environment. The main goal in this experiment is to use proposed design for autonomous take-off and landing to track desired reference trajectory x_d, y_d and z_d. The task is to climb 1.5 m, hover and then land. The evaluation results are depicted in Fig. 14. Due to page constraint, we only present desired position trajectories in x and y direction. We can observe the slight deviation in transient phase due to the presence of position measurement error associated with visual tracking system. With the same setup, we also perform various tests in outdoor and indoor environment for demonstration. These demonstration videos can be watched by visiting the web-site at https://www.youtube.com/watch?v=gvVNctExbY4 and https://www.youtube.com/watch?v=c-6b18dKkJY. Let us now analyze the stability and robustness of the proposed control algorithm for keeping the quadrotor vehicle at desired location. For this, we conducted various tests in indoor and outdoor environment by injecting uncertain external disturbances along with z, ϕ, θ and ψ direction. The goal in these tests is to maintain desired height 1m while the quadrotor can hover around the zero set position. Using these tests, we also made several videos for demonstration. These videos can be watched by clicking the web-site at https://www.youtube.com/watch?v=Msptf5tKCnE and https://www.youtube.com/watch?v=Ol7zdn6R1fg. In view of this demos, we can see that the quadrotor can hover around

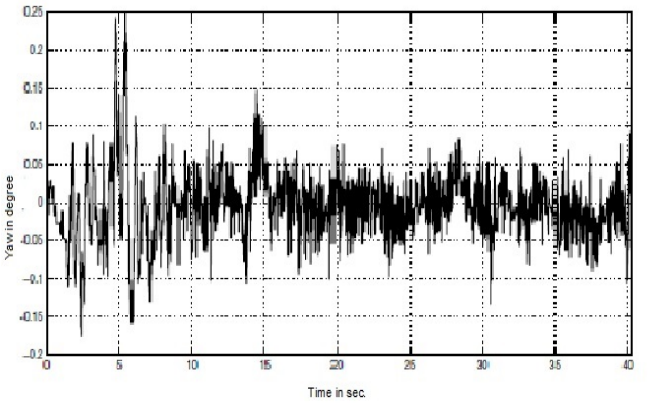

Fig. 13. Figure shows yaw angle ψ in outdoor flying environment.

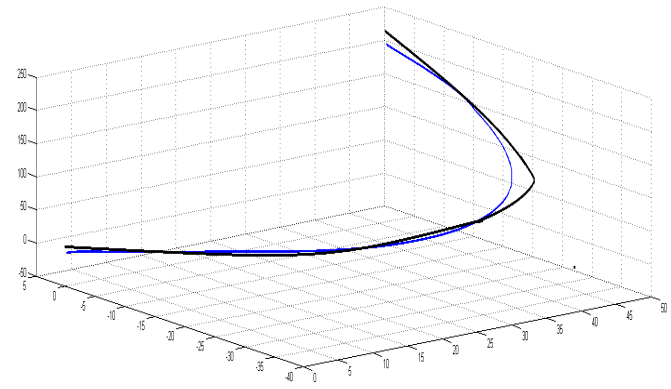

Fig. 14. Actual and desired trajectories of quadrotor UAV in (y, x, t), blue-line (y, x, t) is the actual path and black-line (y, x, t) is the desired path in outdoor flying environment.

the set position with desired height with the presence of the strong disturbances provided by operator along x, y, z, ϕ, θ and ψ direction.

IV. Conclusion

In this paper, we have developed very simple robust control strategy for quadrotor UAV system to deal with the problem associated with uncertainty. Algorithms have designed by combining robust control with adaptive control technique via using Lyapunov function. Compared with other existing nonlinear adaptive backstepping control algorithms, the proposed design is simple and easy to implement as it does not require augmented variable and multiple design steps without a known bound of the uncertainty. Experimental results on actual quadrotor UAV system have presented to demonstrate the theoretical development of this paper. These results showed that the proposed design can ensure the stability and tracking control property of the whole closed loop system for the given bounded uncertainty associated with modeling error and external disturbance.

References

[1] H. Schwartz and S. Islam, An evaluation of adaptive robot control via velocity estimated feedback, In Proceedings on Control and Applications, Montreal, Quebec, May 30-June 1, 125-133, 2007.

[2] A. Das, F. Lewis and S. Subbarao, Dynamic Neural Network based Robust Backstepping Control approach for Quadrotors, *Proc. of the 2008 AIAA Guidance, Navigation and Control Conference and Exibit*, Hawaii, August, 2008.

[3] S. Islam, L. D. Seneviratne and J. Dias, Adaptive tracking control of quadrotor robot vehicle, *In Proc. IEEE/ASME International Conference on Advanced Intelligent Mechatronics*, July8-11, Besanon, France, pp. 441-445, 2014.

[4] D. Gurdan, J. Stumpf, M. Achtelik, K. Doth, G. Hirzinger, and D. Rus, Energy-efficient autonomous four-rotor flying robot controlled at 1 kHz, *In Proc. IEEE International Conference on Robotics and Automation*, Roma, Italy, 361-366, 2007.

[5] E. Altug, J. P. Ostrowski and C. J. Taylor, Quadrotor control using dual cameral visual feedback, *Proceedings of the IEEE International Conference on Robotics and Automation*, 3, 4294-4299, 2003.

[6] G. V. Raffo, M. G. Ortega and F.R. Rubio, Backstepping/Nonlinear H_∞ control for path tracking of a quadrotor unmanned aerial vehicle, *Proceedings of American Control Conference*, seattle, Washington, USA. June, 3356-3361, 2008.

[7] H. K. Khalil, Adaptive output feedback control of nonlinear systems represented by input-output models, *IEEE Transactions on Automatic Control*, 41(2), 177-188, 1996.

[8] L. A. J. Toledo, M. Sigut, and J. Felipe, Stabilization and altitude tracking of a four-rotor microhelicopter using the lifting Operators, *IET Control Theory and Application*, 3(4), 452-464, 2009.

[9] M. Huang, B. Xian, C. Diao, K. Yang and Yu Feng, Adaptive tracking control of underactuated quadrotor unmanned aerial vehicles via backstepping, *American Control Conference*, Baltimore, MD, USA, June 30-July 02, 2076-2081, 2010.

[10] P. E. I Pounds, P. I. Corke and R.E. Mahony, Modelling and control of a large quadrotor robot, *Control Engineering Practice*, 18(7) 691-699, 2010.

[11] P. Castillo, A. Dzul and R. Lozano, Real-Time stabilization and tracking of four-rotor mini rotorcraft, *IEEE Transactions on Control Systems Technology*, 12(4), 510-516, 2004.

[12] S. Bouabdallah and R. Siegwart, Backstepping and sliding-mode techniques applied to an indoor micro quadrotor, *Proceedings of IEEE International Conference on Robotics and Automation*, 2259-2264, 2005.

[13] S. Bouabdallah and R. Siegwart, Full control of a quadrotor, *Proceedings of the EEE/RSJ International Conference on Intelligent Robots and Systems*, USA, 153-158, 2007.

[14] S. Islam, P. X. Liu, A. El Saddik, Robust control of four rotor unmanned aerial vehicle with disturbance uncertainty, *IEEE Transaction on Industrial Electronics*, In press, 2014.

[15] S. Bouabdallah and R. Siegwart, Design and control of an indoor micro quadrotor, Full control of a quadrotor, *Proceedings of the 2003 IEEE International Conference on Robotics and Automation*, New Orleans, USA, 153-158, 2004.

[16] T. Madani and A. Benallegue, Control of a quadrotor via full state backstepping technique, *Proc. of the 45th IEEE conference on Decision and Control*, San Diego, CA, USA, 13-15, 2006.

[17] T. Madani and A. Benallegue, Backstepping control for a quadrotor Helicopter, *Proceedings of the IEEE/RSJ International Conference on Intelligent Robots and Systems*, Beijing, China, 3255-3260, 2006.

[18] T. Madani and A. Benallegue, Backstepping sliding mode control applied to a miniature quadrotor flying robot, *Proceedings of the 32nd Annual Conference of the IEEE Industrial Electronics Society IECON*, Paris, 700-705, 2006.

[19] T. Hamel, R. Mahony and A. Chriette, Visual servo trajectory tracking for a four rotor VTOL aerial vehicle, *Proceedings of the IEEE International Conference on Robotics and Automation*, 2002.

[20] Y. Morel, and A. Leonessa, Direct adaptive tracking control of quadrotor aerial vehicles, *Proc. of the Florida Conference on Recent Advances in Robotics*, 1-6, 2006.

[21] S. Islam, P. X. Liu, A. El Saddik, Nonlinear adaptive control of quadrotor flying vehicle, *Journal of nonlinear Dynamics*, 76(4), 117-133, 2014.

[22] S. Sastry and M. Bosdon, *Adaptive control: Stability, Convergence and Robustness* Printice-Hall, 1989.

[23] Ascending technologies (AscTec) [Online]. Available: http://www.asctec.de.